




# Green Synthesis, Characterization and Antimicrobial Activity of Copper Oxide Nanomaterial Derived from *Momordica charantia*

This article was published in the following Dove Press journal:  
*International Journal of Nanomedicine*

Hina Qamar <sup>1</sup>  
Sumbul Rehman <sup>2</sup>  
Dushyant Kumar Chauhan <sup>1</sup>  
Ashok Kumar Tiwari<sup>3</sup>  
Vikramaditya Upmanyu<sup>3</sup>

<sup>1</sup>Department of Zoology, Chaudhary Charan Singh University, Meerut, Uttar Pradesh, India; <sup>2</sup>Department of Ilmu Advia (Unani Pharmacology), A.K. Tibbiya College, Aligarh Muslim University, Aligarh, Uttar Pradesh, India; <sup>3</sup>Biological Standardization Division, Indian Veterinary Research Institute, Bareilly, Uttar Pradesh, India

**Background:** In the emerging field of nanotechnology, copper oxide (CuO) nanomaterials are considered to be one of the most important transition metal oxides owing to its fascinating properties. Its synthesis from green chemistry principles is gaining importance as next-generation antibiotics due to its simplicity, eco-friendliness, and cost-effectiveness. In the present study, CuO nanorods (CuO NRs) were synthesized from the aqueous fruit extract of *Momordica charantia* and characterized using different analytical techniques. Further, the biomedical therapeutic potential was evaluated against multi-drug resistant microbial strains.

**Materials and Methods:** To synthesize CuO NRs, 0.1M of CuSO<sub>4</sub>·5H<sub>2</sub>O solution was added to aqueous extract of *Momordica charantia* in a 1:3 (v/v) ratio (pH=11) and heated at 50°C followed by washing and drying. The synthesized CuO NRs were subjected to characterization using different analytical techniques such as UV visible spectroscopy, zeta sizer equipped with zeta potential, Fourier transform infrared spectroscopy (FTIR), X-ray diffraction (XRD), scanning electron microscopy (SEM) equipped with energy-dispersive X-ray spectroscopy (EDS) and transmission electron microscopy (TEM). Further, the application as a biomedical therapeutic potential was evaluated in vitro using well diffusion method against eleven multidrug-resistant clinical bacterial strains, a fungus- *Trichophyton rubrum* and in ovo against the R<sub>2</sub>B virus using haemagglutination (HA) test.

**Results:** Characterization was preliminarily done by the spectral study that confirms the absorbance band at 245nm. FTIR analysis at 628 cm<sup>-1</sup> peak identified copper oxide vibration. SEM analysis revealed agglomerated particle clusters. However, with TEM clear nanorods of average diameter of 61.48 ± 2 nm were observed. EDAX confirmed CuO formation while XRD showed a typical monoclinic structure with 6 nm crystallite size. Biological screening of CuO NRs showed significant results against both in vitro and in ovo methods. Significant inhibitory activity (p<0.0001) was noted against most of the resistant human pathogenic strains including both Gram-positive and Gram-negative bacteria. The highest efficacy was observed against *Bacillus cereus* with a 31.66 mm zone of inhibition. Besides, the therapeutic potential of CuO NRs against *Corynebacterium xerosis*, *Streptococcus viridians* and R<sub>2</sub>B strain of Newcastle disease is reported for the first time.

**Conclusion:** Based on the present results, it could be expected that green synthesized CuO NRs would find potential applications in the field of nanomedicine.

**Keywords:** copper oxide nanorods, CuO NRs, biosynthesis, antibacterial, antifungal, antiviral, *Trichophyton rubrum*, multidrug-resistance, TEM, R<sub>2</sub>B Newcastle disease virus

Correspondence: Dushyant Kumar Chauhan  
Department of Zoology, Chaudhary Charan Singh University, Meerut 250001, Uttar Pradesh, India  
Tel +91 941 270 8983  
Email drdushyant.zoology@gmail.com

## Introduction

Worldwide, the use of nanomaterial in the biomedical field has attracted the increasing interest of researchers owing to their unique property when interacting with cells and tissues at the molecular level with a high degree of specificity and improved efficacy to combat infectious diseases.<sup>1</sup> Their small size, design flexibility and large surface-to-volume ratio make these materials of intense use.<sup>2,3</sup> It is a known fact that metal oxide at the nanoscale exhibits improved properties and thus during the past decade extensive research on different metal oxide nanomaterials such as copper oxide nanoparticles and nanorods, have been carried out to explore their applications in different interdisciplinary fields.<sup>4,5</sup>

Copper oxide nanomaterials have been gaining interest as nanomaterial due to their unique optical, thermal, electrical, chemical and biological properties.<sup>6,7</sup> These properties impart a wide range of their applications in different fields from the formation of sensors, storage devices, supercapacitors and infrared filters to the health and environment sector.<sup>6,8</sup> Also, the antimicrobial activity of CuO nanomaterial has made them strong candidates to be used as therapeutic agents.<sup>9</sup> At present, researchers are facing a major challenge in the healthcare sector to combat drug resistance. In this regard, day-by-day several improved synthesis strategies are developing that includes physical, chemical and biological processes.<sup>10</sup> Though synthesis of CuO nanomaterial is cost-effective as compared to silver (Ag), gold (Au) and platinum (Pt) nanoparticles, but to attain its stability is still a challenging task.<sup>11,12</sup> Many studies have been performed on the synthesis of CuO nanomaterial which include vapor deposition<sup>13</sup> to electrochemical reduction,<sup>14</sup> radiolysis reduction,<sup>15</sup> thermal decomposition<sup>16</sup> and chemical reduction.<sup>17</sup> But these strategies are associated with the contamination issues and harm ecosystems as well as human health.<sup>5</sup> Thus, to overcome these shortfalls, the principle of green chemistry utilizing natural origin sources such as plants and microbes for the synthesis process may prove to be a potential solution.<sup>12</sup>

In the present study, an attempt has been made to develop an eco-friendly, cost-effective technique for the synthesis of CuO nanorods (CuO NRs) by reducing Cu<sup>2+</sup> ions in the copper sulfate solution using *Momordica charantia* (Bitter gourd) fruit extract. The characterization of CuO NRs was done by standard physiochemical techniques. Further, the biomedical applications of green synthesized CuO NRs were evaluated against multidrug-resistant bacterial strains

that threaten modern medicine where common infections could become more deadly. Next to bacterial infections, CuO NRs were screened for antifungal activity against *Trichophyton rubrum*, which causes a superficial dermatophyte infection that has increased to an alarming level in the last few years due to the resistance developed to many conventional antidermatophytic agents having an azole group.<sup>18</sup> Dermatophytes are pathogenic fungi belonging to the keratinophilic group that requires keratin for their growth and infects the keratinized tissues of humans and animals such as hairs, nails, and skin.<sup>19</sup> Though several methods have been availed to control and prevent the growth of fungal cells yet there is a vital need to explore this field utilizing nanomedicines.<sup>20</sup> Preceding, the antiviral activity of CuO NRs was also evaluated against R<sub>2</sub>B strain of Newcastle disease virus (NDV) which is a fast-growing, single-stranded RNA avian paramyxovirus that causes a contagious bird disease which incurs huge economic loss throughout the world to poultry farmers by inducing mortality, low egg production and reduced amount of dietary proteins. Studies report that NDV causes conjunctivitis in humans especially to the people who get exposed to poultry farms.<sup>21,22</sup>

## Materials and Methods

### Materials

Copper (II) sulfate pentahydrate (CuSO<sub>4</sub>·5H<sub>2</sub>O) and Dimethyl sulfoxide (DMSO) were obtained from Sigma-Aldrich. Nutrient agar, nutrient broth medium and antimicrobial disks were purchased from Hi-media Labs, Mumbai, India. The clinical isolates of bacterial and fungal cultures were kindly provided by Microbiology Lab, Department of Ilmu Advia and Jawaharlal Nehru Medical College and Hospital, Aligarh Muslim University, Aligarh and R<sub>2</sub>B strain of NDV from Indian Veterinary Research Institute, Izzatnagar, Bareilly (U.P). All bacterial strains were resistant to Cefixime, Amoxycylav, Cefotaxime, Methicillin and Ampicillin antibiotics.

### Methods

#### Preparation of Extract

Fresh fruits of *Momordica charantia* (MC) were procured from the local market. After thorough washing, the fruit was ground to reduce the particle size and was subjected to extraction by the reflux method using soxhlet apparatus to obtain crude aqueous extract.<sup>23</sup> To prepare the aqueous extract, 1:10 w/v of the mixture in distilled water was

taken and heated at 50 °C for 40 min. The extract was filtered and stored at 4 °C until further use.

### Green Synthesis of CuO NRs

To synthesize CuO NRs, Mary, et al, 2019 protocol with slight modifications was followed. Briefly, 0.1M of CuSO<sub>4</sub>.5H<sub>2</sub>O solution was added to aqueous extract of *M. charantia* (AE-MC) in a 1:3 (v/v) ratio followed by pH adjustment to 11 by sodium hydroxide pellet. Then, the solution was heated at 50 °C till the color of solution changes to brown which might indicate the formation of CuO NRs. The solution containing synthesized CuO NRs was washed three times, each repeat followed by centrifugation at 5000 rpm for 10 minutes. Finally, the pellet was collected, dried and stored at 4 °C till further use.<sup>24</sup>

### Physiochemical Characterization of CuO NRs

To confirm the formation of CuO NRs different physiochemical characterization techniques were used.

### UV-Vis Spectroscopy

Optical properties were analyzed by visualization of peaks obtained from UV-Vis spectral scan from 200 nm to 800 nm in a UV-Visible spectrophotometer (Motras Scientific; UV Plus).

### Zeta Sizer and Zeta Potential

For determining the size of CuO NRs, in aqueous medium zeta size and zeta potential were measured using a Zetasizer (Nano-ZS, Model ZEN3600).

### Fourier Transform Infrared Spectroscopy

For the fourier transform infrared spectroscopy (FTIR) analysis sample was grounded with KBr pellet and analyzed on a Perkin Elmer (Model: Spectrum Two) with spectrum recorded in the range of 400–4000 cm<sup>-1</sup>.

### X-Ray Diffraction

X-ray diffractometer (XRD, Model: Mini Flex II; Make: Rigaku) was used to determine the crystallite size, structure and crystallinity of nanoparticle with Cu-K<sub>α</sub> radiations ( $\lambda = 0.154$  nm) in 2 $\theta$  range from 20° to 80° followed by data analysis in PowderX software. The mean size of nanocrystals for the particle was determined from the diffraction peaks corresponding to the most intensive reflections according to the JCPDS (Joint Committee on Powder Diffraction Standards) database and International Centre for Diffraction Data (ICDD).

### Transmission Electron Microscopy

Transmission electron microscopy (TEM) analysis was done using a 200kV JEOL transmission electron microscope (JEOL Ltd. Tokyo, Japan) to determine the size of the synthesized particles. For TEM analysis, the sample was prepared by adding 20  $\mu$ L of CuO nanomaterial solution on a Cu grid, dried at room temperature and subsequently analyzed under the microscope with different magnifications.

### Scanning Electron Microscopy and Energy-Dispersive X-Ray Spectroscopy

The morphology to determine shape lattice and chemical composition of synthesized nanoparticles were examined by scanning electron microscope (SEM; Model No. JSM 6510LV, Make-JEOL, Japan) equipped with energy dispersive X-ray spectrometer (EDSX) followed by microscopic imaging performed from 1000X to 30,000X with 0.5–1 $\mu$ m resolution at 15kV.

### Biological Screening of CuO NRs

#### In vitro Antimicrobial Assay of CuO NRs Against Multidrug-Resistant Bacterial Strains

The susceptibility of CuO NRs against multidrug-resistant bacterial strains was determined using Kirby-Bauer's disk diffusion and agar well diffusion method according to CLSI (Clinical Laboratory Standard Institute) Guidelines (2009).<sup>25,26</sup> Seven Gram-positive (*Staphylococcus aureus*, *Streptococcus mutans*, *Streptococcus pyogenes*, *Streptococcus viridans*, *Staphylococcus epidermidis*, *Corynebacterium xerosis*, and *Bacillus cereus*) and four Gram-negative (*Escherichia coli*, *Klebsiella pneumonia*, *Pseudomonas aeruginosa*, and *Proteus vulgaris*) multi-drug-resistant clinical bacterial strains were used. About 50 $\mu$ L of the test sample (concentration of CuO NRs 1.25 mg/50  $\mu$ L DMSO) was used against each strain swabbed on nutrient agar plates followed by incubation at 37°C for 24 hrs. DMSO was used as negative control while 50 $\mu$ L aqueous extract of *M. charantia* was used as positive control and 10 $\mu$ g Streptomycin disk for Gram-positive and 10 $\mu$ g Norfloxacin disk for Gram-negative strains were used as standard: positive control. Antimicrobial activity was assessed using a zone of inhibition (ZOI) measured after the incubation period against each tested micro-organisms.

#### In vitro Antifungal Assay of CuO NRs

Antifungal activity of CuO NRs against *Trichophyton rubrum* was determined using agar well diffusion method.<sup>27</sup>

Briefly, Sabouraud dextrose agar culture media plates were prepared, inoculated with the *T. rubrum* and incubated at 25°C for 15 days for fungus growth. After 15 days, wells were punched in the agar plate using a core-borer and 100µL CuO NRs dissolved in DMSO was instilled in a well. The plates were left for 1 h at 37 °C to allow the diffusion of the test sample and then incubated at 25 °C for a week. DMSO was used as negative control while 50µL aqueous extract of *M. charantia* was used as positive control and 10µg Fluconazole disk was used as standard. After the incubation period, the zone of inhibition was measured against tested fungus.

### In Ovo Antiviral Activity of CuO NRs

#### Virus Cultivation and EID<sub>50</sub> Calculation

In ovo antiviral screening of the CuO NRs was carried out in 9–10 day old sterilized embryonated chicken eggs through allantoic cavity route on R<sub>2</sub>B strain of Newcastle Disease Virus (NDV) and their efficacy was assessed by haemagglutination (HA) test.<sup>28</sup> Firstly, NDV was propagated in eggs. Then, to determine the virus titer, embryo infectious dose (EID<sub>50</sub>) following embryo % mortality and % viability testing was evaluated (Table 1).<sup>29</sup> EID<sub>50</sub> was calculated using a mathematical technique devised by Reed and Muench.<sup>30</sup> To study antiviral activity, two different combinations of CuO NRs concentrations with determined EID<sub>50</sub>/mL of virus inoculum were used. Working NDV concentration was prepared by diluting the NDV stock to 1:2000 in phosphate buffer saline (PBS) and injecting 0.1mL of inoculum in the allantoic cavity by perching the hole at egg air sac space. Two different doses: first d<sub>1</sub>=50µg/mL and second d<sub>2</sub>=100µg/mL of CuO NRs were prepared dissolved in 1% DMSO.

Eggs were grouped into four, each carrying 5 eggs as follows:

Group A:Negative control [1mL of 1% DMSO]

Group B:Positive control [1mL of NDV inoculum]

Group C:Low dose- Nanoparticle treated [0.9mL of CuO NRs (50µg/mL) followed by 0.1mL NDV inoculum]

Group D:High Dose-Nanoparticle treated [0.9mL of CuO NRs (100µg/mL) followed by 0.1mL NDV inoculum]

The treated eggs were incubated at 37°C for 96 hours followed by regular monitoring for embryonic development and viability status at every 24-hour interval. After 96 hours, all eggs were chilled for an hour at 4°C to kill the embryo and evaluated for antiviral activity by haemagglutination assay.

#### Haemagglutination Test

To confirm the presence of NDV in allantoic fluid, the haemagglutination test using 96 well microtiter plate was carried out.<sup>28</sup> Allantoic fluid from each egg was collected separately. 50µL PBS solution was added in each well of the microtiter plate followed by the addition of 50µL of 0.45µ filtered allantoic fluid in two-fold dilutions in subsequent wells. Next, 25µL 10%RBCs was added to each well and left for 45 min at room temperature. After the incubation period, the plate was observed for any visible agglutination reaction visualized as a sharp button or diffused film. Three separate wells were treated as control as follows:

Self-Control: 50µL PBS+25µL 10%RBCs (for auto-agglutination)

Negative Control: 50µL allantoic fluid lacking NDV +25µL 10%RBCs

Positive Control: 50µL allantoic fluid having NDV+ 25µL 10%RBCs

### Statistical Analysis

The experiment was performed in triplicates, Mean ± SEM (S.D) was compared with the standard used and analyzed statistically using graph-paid instat Dataset1.ISD software by Tukey Kramer Comparison test, One way ANOVA.

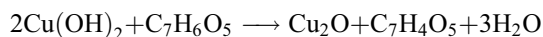
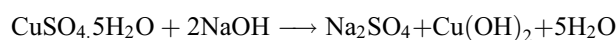
**Table 1** In Ovo Evaluation of CuO NRs Antiviral Activity

Groups				Mean±SEM (SD)	% Viability
Untreated	A	Negative control	1mL of 1% DMSO	4.66±0.3 (0.57)	100
	B	Positive control	1mL of NDV inoculum	0±0 (0)	0
Treated	C	CuO NRs treated (Low dose)	0.9mL CuO NRs (50µg CuO NRs concentration dissolved in 1mL 1% DMSO + 0.1mL NDV inoculum)	2.66±0.88 (1.5)	53.2
	D	CuO NRs treated (High dose)	0.9mL CuO NRs (100µg CuO NRs concentration dissolved in 1mL 1% DMSO + 0.1mL NDV inoculum)	4±0.5 (1.0)	80

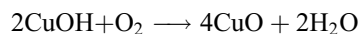
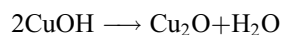
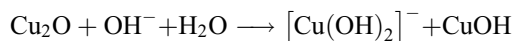
## Results and Discussion

### Green Synthesis of CuO NRs and UV-Vis Spectroscopic Analysis

The present study deals with the rapid green synthesis of CuO NRs from fruit extract of *Momordica charantia*. There are a plethora of studies that reported the presence of various bioactive compounds in *M. charantia* such as triterpenes, alkaloids, steroids, phenols, etc. to list a few.<sup>31</sup> In the present study, the mechanism of CuO NRs synthesis can be hypothesized and explained by using the phenolic content of fruit extract of *M. charantia* as they are known to have the high reducing ability.<sup>32,33</sup> It is well documented that the gallic acid is present as one of the key phenolic components in *M. charantia* fruit extract which might facilitate the reduction of Cu(OH)<sub>2</sub> to nano-sized CuO.<sup>34</sup> During the reaction, when pH is increased in the range of 11, the color of reaction changes from blue to brown and then to black.<sup>35</sup> The changes in the color may be understood in terms of the reaction between copper (II) sulfate pentahydrate and sodium hydroxide to form copper (II) hydroxide (blue), which in turn reacts with the gallic acid resulting in the formation of dehydrogallic acid and copper (I) oxide (brown).<sup>36</sup>



However, as reaction proceeds with time, the copper (I) oxide was formed and finally CuO nanoparticles formation occur by a series of following reactions (Figure 1).<sup>35-37</sup>



Color changed from blue to brown due to excitation of surface Plasmon resonance and presence of polyphenolics as antioxidant source arising as a result of  $\pi \rightarrow \pi^*$  transitions indicated the synthesis of CuO NRs.<sup>4</sup> Further, the absorption spectrum recorded at 200–600 nm showed a single absorbance peak at 246 nm corresponded to the characteristic absorbance band of CuO NRs which was in accordance with previous studies reported (Figure 2).<sup>4,36</sup>

### Zeta Size and Potential of CuO NRs

An average hydrodynamic diameter of CuO NRs was measured by Zetasizer using dynamic light scattering

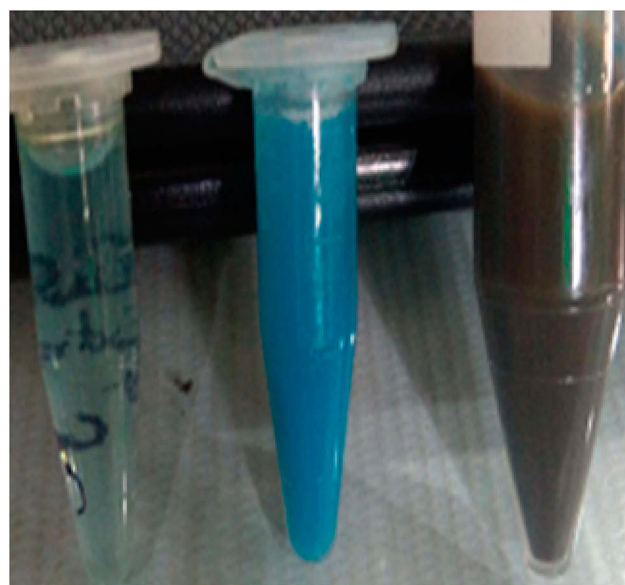


Figure 1 Sequential color change during the formation of CuO nanorods.

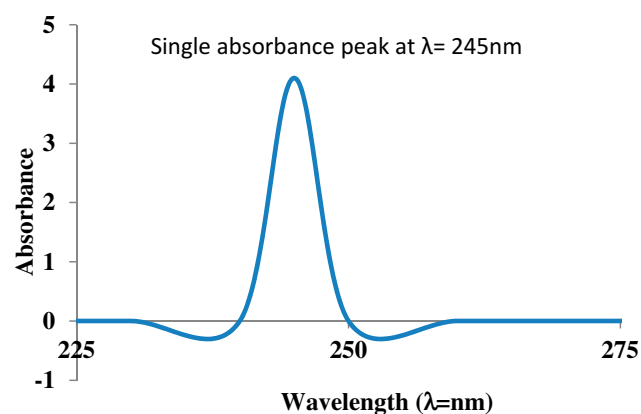


Figure 2 UV visible spectral analysis of CuO nanorods.

(DLS) and was found to be  $90 \pm 5$  nm (Figure 3). DLS is widely used for determining the diameter of suspended particles hydro dynamically based on the Brownian movement. It is the particle diffusion behavior within any fluid and is measured by the fluctuations in light intensity that passes through a colloidal solution as a function of time.<sup>37</sup> Further, zeta potential is considered as a measure of charges on the surface of nanoparticles. It indicates the stability of colloidal dispersions. Colloids that have high zeta potential are electrically more stable than colloids with low zeta potential that tends to coagulate. The stability is maintained by potent repulsive forces among the ultrafine particles.<sup>38</sup> To measure zeta potential using electrophoretic light scattering, nanoparticles were dispersed in water. The results showed zeta potential to be  $-7.23$

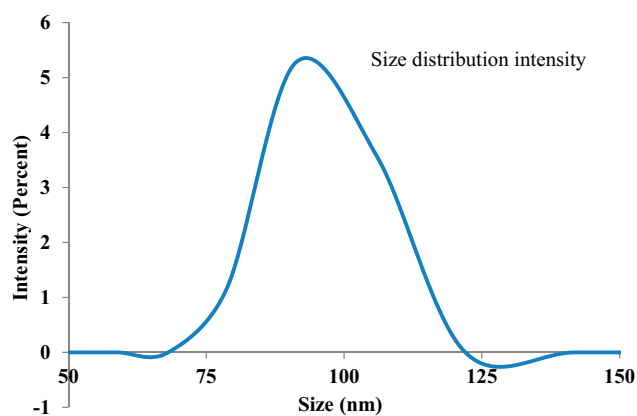


Figure 3 Zeta sizer measurement of CuO nanorods.

mV. Lower zeta potential value indicates the presence of thin coating of *M. charantia* aqueous extract over the nanorods that might result in colloidal instability and agglomeration. Furthermore, the negative value indicates the formation of hydroxyl groups on the surface of particles upon dispersion in water.<sup>38</sup>

### FTIR Analysis of CuO NRs

FTIR spectral analysis of CuO NRs showed different peaks at 459–487.3  $\text{cm}^{-1}$ , 590.4–628.2  $\text{cm}^{-1}$ , 1087.2–1125  $\text{cm}^{-1}$ , 1377.9–1434.6  $\text{cm}^{-1}$ , 1612.8–1668.2  $\text{cm}^{-1}$ , 2071.8  $\text{cm}^{-1}$ , 2700–2954  $\text{cm}^{-1}$  and 3384–3534.3  $\text{cm}^{-1}$  (Figure 4). The broad peak observed at 3384–3534.3  $\text{cm}^{-1}$  corresponds to

the O–H and N–H bond stretching vibrations. The vibrations might be due to phenolic compounds present in the solution.<sup>39</sup> The small peak at 2071.8  $\text{cm}^{-1}$  corresponds to the stretching vibrations of the compounds containing C $\equiv$ N bonds. The sharp peak at 1612.8–1668.2  $\text{cm}^{-1}$  corresponds to the presence of C=N or C=O stretching. Likely, peak at 1377.9–1434.6  $\text{cm}^{-1}$  denote sp<sup>3</sup> C–H bending or acyl C–O (or phenol C–O) stretching and 2700–2954  $\text{cm}^{-1}$  denotes C–H stretching. Furthermore, the peak at 1087.2–1125  $\text{cm}^{-1}$  denotes alkoxy C–O. The unsaturated C–H bending appears under 1000  $\text{cm}^{-1}$  that might be due to the presence of bioactive phytochemicals such as triterpenes, proteins, steroids, carbohydrates, alkaloids and other compounds in the solution. These compounds might impart capping which helps in maintaining the stability of CuO NRs. Moreover, a sharp peak found in the infrared spectrum at low frequencies at 590.4–628.2  $\text{cm}^{-1}$  corresponds to CuO vibrations which were in accordance with earlier reports.<sup>40</sup>

### XRD Analysis of CuO NRs

The microcrystalline structure of CuO NR was analyzed using the XRD technique. The graph was prepared using PowderX software. As shown in Figure 5, the characteristic XRD peaks were observed at 32.64, 35.1, 38.9, 48.9, 52.0, 58.46, 62.9, 65.94 and 67.96 corresponding to 110, 002, 111, 202, 020, 202, 113, 311 and 113 reflections respectively which indicate the formation of typical monoclinic CuO

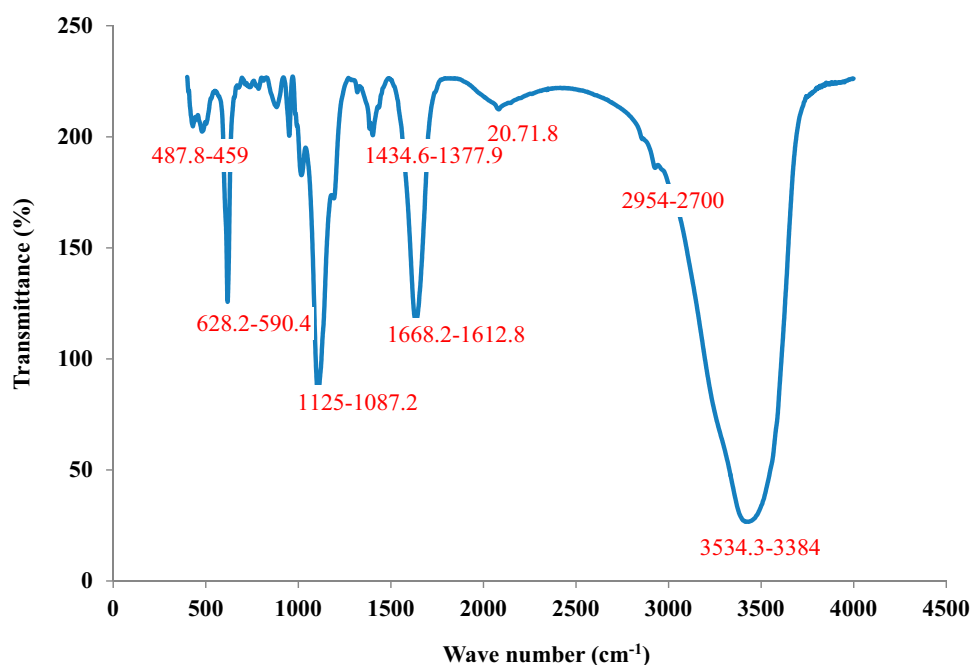
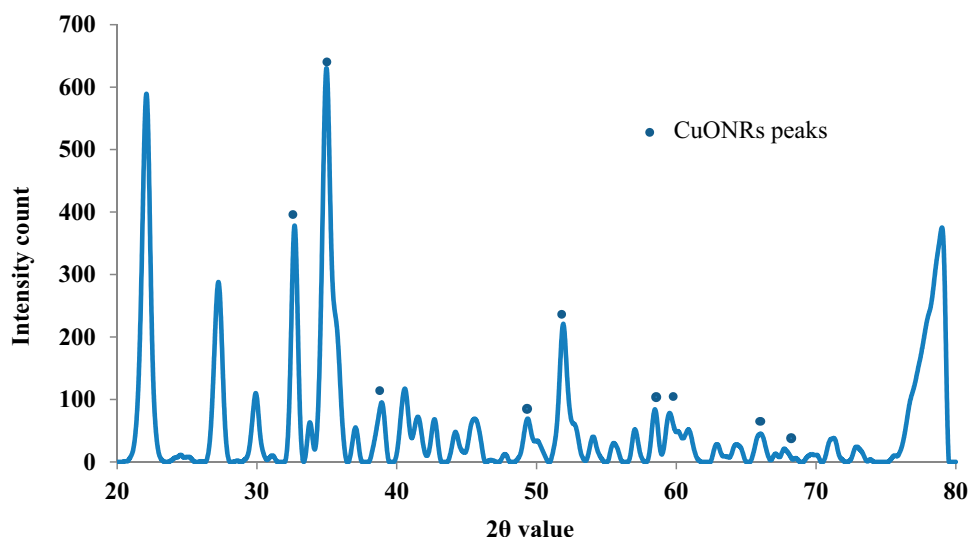


Figure 4 FTIR analysis of CuO nanorods.



**Figure 5** XRD pattern determination of CuO nanorods.

NR structure and are in agreement with the standard values reported by the JCPDS card no. 801268 and ICDD card no. 801916 which was in accordance with previous studies reported.<sup>40,41</sup> However, other peaks are also denoted in the figure. The average crystallite size was calculated to be 6 nm using Debye Scherrer's equation.

$$D = K\lambda / (\beta \cos\theta)$$

Where D is an average particle size (nm), K is the constant and equals to 0.94,  $\lambda$  is the wavelength of X-ray radiation,

$\beta$  is full-width at half maximum (FWHM) of the peak in radians and  $\theta$  is the diffraction angle (degree).

### SEM/EDS Analysis of CuO NRs

Microscopic SEM analysis revealed that particles might be spherical. A clear morphology could not be depicted as exhibited agglomeration and clumped to form clustered particles (Figure 6).<sup>42,43</sup> The EDX spectroscopy was applied to quantify the elemental composition of synthesized nanoparticles. The spectrum of CuO NRs given in

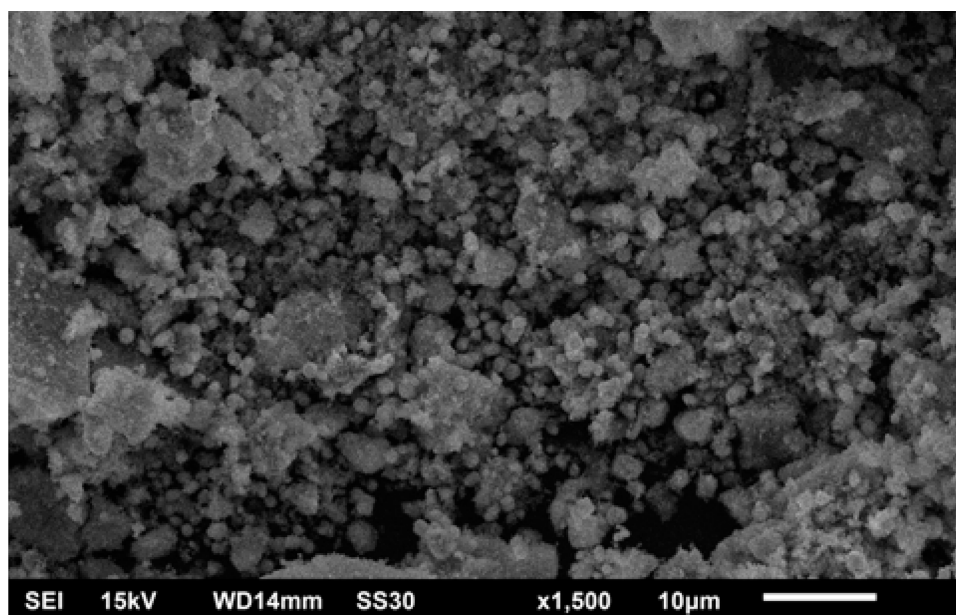


**Figure 6** SEM analysis of CuO nanorods.

Figure 7 confirms the existence of Cu, O and C. The peak around 0.5 keV belongs to the binding energy of oxygen (OK $\alpha$ ); while peaks located at binding energies of 1, 8 and 9keV correspond to CuL $\alpha$ , CuK $\alpha$ , and CuK $\beta$ , respectively. Additionally, a peak at 0.25keV corresponding to carbon (CK $\alpha$ ) was also reported. The percentage of Cu, O, and C present in CuO NRs was found to be 54.51%, 31.50%, and 13.99% respectively. The appearance of a carbon peak in the sample verified the presence of carbon-based stabilizers or it may be due to carbon tape used during the process.<sup>44</sup>

## TEM Analysis of CuO NRs

TEM analysis revealed well dispersed rod-shaped nanoparticles within the range of  $61.48 \pm 2$  nm in diameter and 400–500 nm in length (Figure 8). The figure shows that nanoparticle distributions are compatible with the Gaussian distribution, noting that the distribution is skewed toward a small size. The most common nanoparticle size was 60 nm and the range of nanoparticle sizes was between 50–57 nm.

As shown by the selected area electron diffraction (SAED) pattern it is clear that the prepared nanoparticles are in a well defined crystalline form identical to the single-phase. It indicates a reflection of the monoclinic CuO structure (Figure 8B) which is in accordance with the XRD pattern as mentioned above. The TEM results mentioned were in consistent with the previous studies reported.<sup>45,46</sup>

## Antimicrobial Analysis of CuO NRs

In the present study, antibacterial preventive and antifungal curative efficacy of green synthesized CuO NRs was

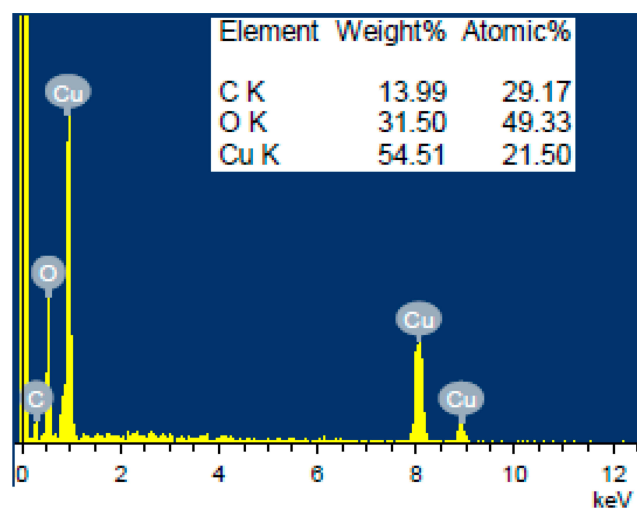
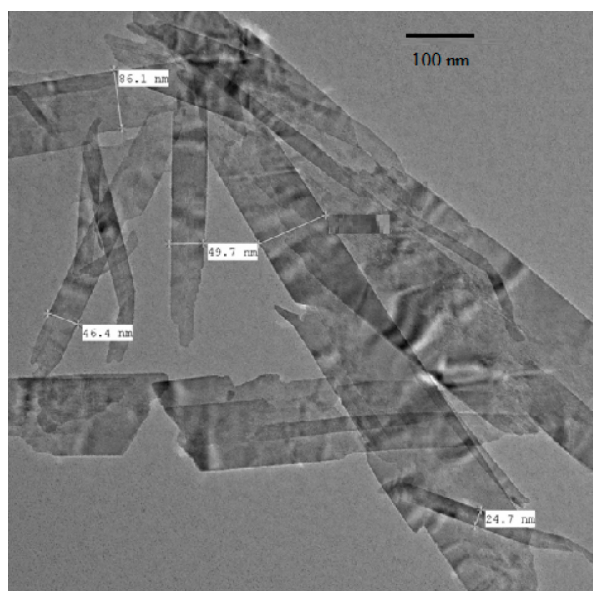


Figure 7 EDS analysis of CuO nanorods.

analyzed using agar well diffusion method which was in accordance with previous studies reported.<sup>20,41</sup>

The antibacterial activity of CuO NRs was evaluated against both Gram-positive and Gram-negative multidrug-resistant bacterial strains by measuring the zones of inhibition (ZoI) (Table 2). The efficacy of CuO NRs for all strains was found to be significant as compared to the standard drug (Figure 9) with  $p < 0.0001$  in most of the cases. The aqueous extract of *M charantia* did not show any activity. The highest efficacy was observed against *Bacillus cereus* with a 31.66 mm zone of inhibition. The results for antifungal activity were also satisfactory for *Trichophyton rubrum* and ZoI was found to be 12 mm which is considered moderately significant (Figure 10). It's observed that the zone of inhibition was less in fungi when compared with bacteria. This is because the fungal cell wall is more firm as it is made up of chitin, comprising of polysaccharides having N-acetylglucosamine and a nitrogen group. Thereby, not allow easy passage of CuO NRs from the outer layer of the cell wall to the inner layer. However, the cell wall of bacteria is made up of peptidoglycan (a polymer having sugars and amino acids), which is less firm and allow easy passage of CuO NRs when compared with fungi. Besides, among the bacterial strains, the antibacterial activity of CuO NRs was found more effective for Gram-positive bacteria in comparison to Gram-negative. Previous studies reported that CuO NRs penetrate inside the bacterial cell due to the changes in membrane morphology that significantly increases cell permeability and affect transport via plasma membrane which results in cell death.<sup>47,48</sup> To date, different mechanisms responsible for the antibacterial activity of CuO NRs have been reported. These include the generation of reactive oxygen species, protein oxidation, lipid peroxidation, destruction of the cell membrane and DNA degradation in bacterial cells.<sup>49</sup> Moreover, the antibacterial activity of nanoparticles depends on its shape, size and oxidation number.<sup>49</sup> In the present study, nanorods have large surface to volume ratio to interact with the cell membranes of microorganisms and ceases their growth. It was also observed that the antimicrobial efficacy of CuO NRs when evaluated after 4 months showed the same ZoI which suggests that CuO NRs efficacy to kill microbes does not decrease with time. Noteworthy, the antifungal activity of CuO NRs against the *Trichophyton rubrum* showed significant results ( $p < 0.0001$ ) when compared to standard drug fluconazole which is almost resistant to *T. rubrum*. They are safe and more acceptable topically, as they have a greater affinity toward amines and carboxyl groups on fungal cell surfaces and their extremely large surface area provides better contact with the fungus. Also, copper ions released

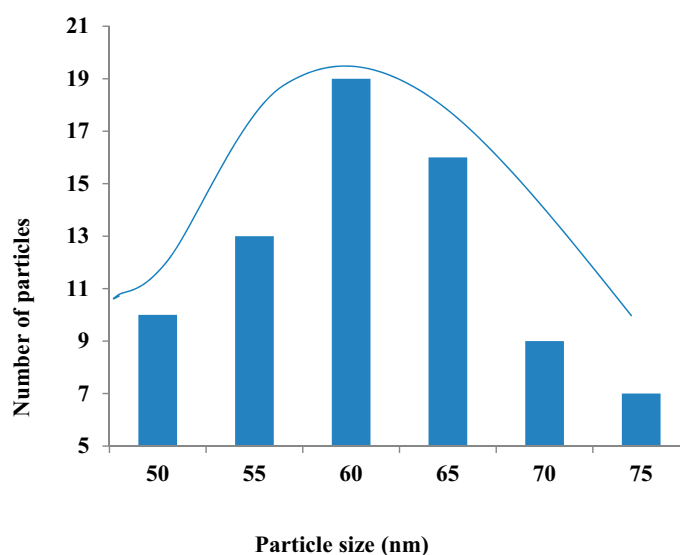




**A** TEM analysis depicting rod-shaped structures



**B** SAED pattern of CuO NRs



**C** Statistical analysis of synthesized CuO NRs

**Figure 8** TEM analysis of CuO nanorods.

**Notes:** (A) TEM analysis depicting rod-shaped structure. (B) SAED pattern of CuO NRs. (C) Statistical analysis of synthesized CuO NRs.

during the process may bind with DNA molecules and disrupt the helical structure, resulting in the lysis of dermatophytic cells.<sup>50</sup> Though several biochemical processes got disrupted when copper ions penetrate inside the cells. Further, studies are required to get ensure the mechanism by which nanoparticles exhibit antifungal activity.<sup>51</sup> It can be assumed that the novel pathways and targets that shall be considered while screening antifungal drugs may include calcineurin, RAS and

sphingolipid synthesis, trehalose, metabolic glyoxylate specifically the enzyme isocitrate lyase, mitogen-activated protein (MAP) kinase, high-osmolarity glycerol (HOG), cell wall target 3-phosphoinositide-dependent protein kinase 1 (Pdk1) and an inhibitor VCN-01 of calcium signaling.<sup>52</sup> Based on the results obtained, the green synthesized CuO NRs can be applied in combination with a lotion or a cream-based product as they have a size greater than 30nm, which is considered safe

**Table 2** In vitro Antimicrobial Assay Readings Against Various Multidrug Resistant Microbial Strains

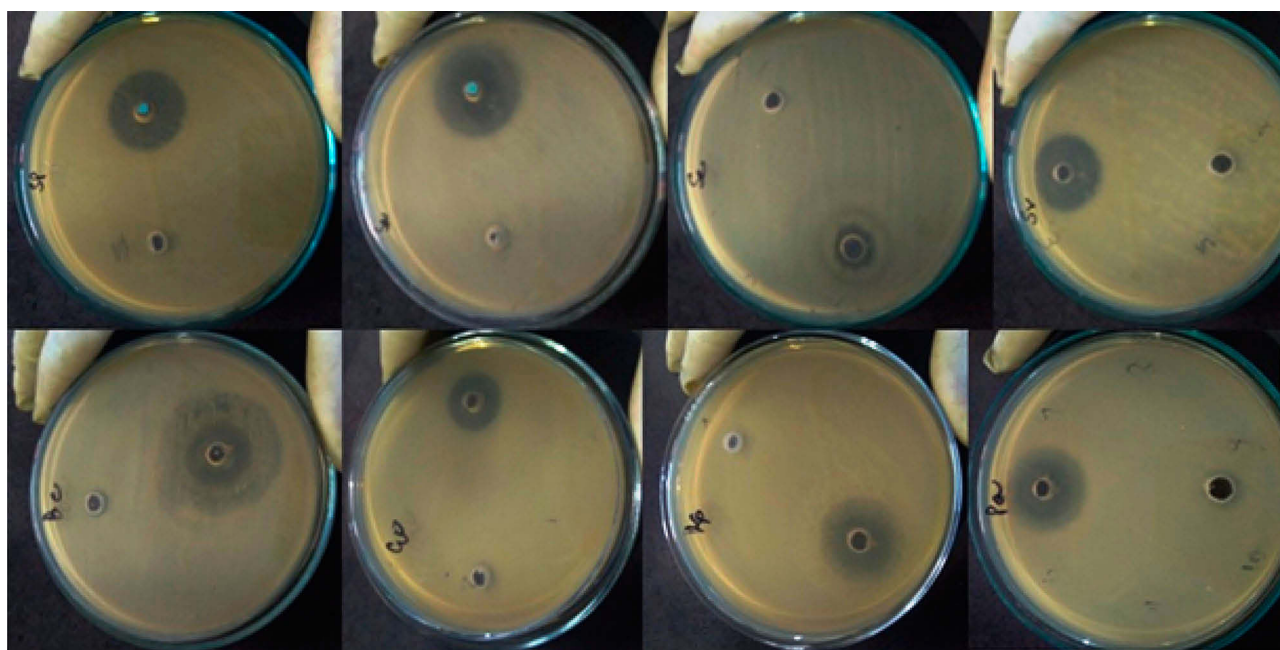
Name of Microbial Strains		Zone of Inhibition (in mm) Results Expressed as Mean±SEM (SD)			
		CuO NRs	Positive Control	Negative Control	P value
Gram positive bacteria	<i>Staphylococcus aureus</i>	28.66±0.66(1.15)	17.66±0.33(0.57)	6.66±0.33(0.57)	<0.0001
	<i>Streptococcus mutans</i>	28.66±0.33(0.5)	28±0.33(0.57)	6.33±0.33(0.57)	<0.0001
	<i>Streptococcus pyogenes</i>	25.66±0.66(1.15)	23±0.83(0.57)	6.33±0.33(0.57)	<0.0001
	<i>Streptococcus viridians</i>	27.33±0.33(0.57)	16.33±0.33(0.57)	6.33±0.33(0.57)	<0.0001
	<i>Staphylococcus epidermidis</i>	23±2.0(3.4)	7.33±0.03(0.57)	6.33±0.33(0.57)	<0.0001
	<i>Corynebacterium xerosis</i>	28.66±5.66(9.8)	19±0.63(0.57)	6.33±0.33(0.57)	0.0085
	<i>Bacillus cereus</i>	31.66±1.2(2.08)	15±0.66(1.15)	6.33±0.33(0.57)	<0.0001
Gram negative bacteria	<i>Escherichia coli</i>	25.33±5.3(9.2)	20±0.33(0.57)	6.66±0.33(0.57)	0.013
	<i>Klebsiella pneumonia</i>	24.66±2.6(4.5)	32±0.33(0.57)	6.33±0.33(0.57)	<0.0001
	<i>Pseudomonas aeruginosa</i>	25.66±2.33(4.04)	14±0.63(0.57)	6.33±0.33(0.57)	0.002
	<i>Proteus vulgaris</i>	26.33±2.18(3.78)	16.33±0.33(0.57)	6.33±0.33(0.57)	<0.0001
Fungus	<i>Trichophyton rubrum</i>	12.54±0.33(0.57)	6.33±0.33(0.57)	6.33±0.33(0.57)	<0.0001

for human health and does not enter the bloodstream through the skin.<sup>20</sup> Due to a high incidence of disease recurrence and other side effects, CuO NRs can be considered as a better solution.<sup>20,53</sup>

### Antiviral Analysis of CuO NRs

In the present study, titration was done to measure infectious NDV concentration in the suspension (Table 3). The embryo infectious dosage (EID<sub>50</sub>) that killed 50% of NDV treated

eggs was calculated by applying the Reed and Muench formula (1938) and was found to be 10<sup>7.5</sup> per mL. After examining EID<sub>50</sub>, the determined EID<sub>50</sub>/mL of virus inoculum has been used against each concentration of CuO NRs to check the antiviral activity (Figure 11). Following 96 hrs of incubation, it was observed that no embryo death occurred in the negative control. Further, 53.2% viability occurred in 50 µg/mL concentrations of CuO NRs treated eggs and 80% in 100µg/mL concentrations of CuO NRs treated eggs (Table 1). Based on

**Figure 9** In vitro antibacterial activity of CuO nanorods.

**Table 3** Calculation of EID<sub>50</sub>

Dilution of NDV	No. of Eggs	Mortality				Accumulated Numbers			% of Mortality= A/A+B X 100	% of Viability= B/A+B X 100
		24 h	48 h	72 h	96 h	Infected eggs (A)	Noninfected eggs (B)	Total (A+B)		
10 <sup>-1</sup>	5	3	2	0	0	5	0	5	100	0
10 <sup>-2</sup>	5	2	1	1	1	5	0	5	100	0
10 <sup>-3</sup>	5	2	1	2	1	5	0	5	100	0
10 <sup>-4</sup>	5	0	1	2	2	5	0	5	100	0
10 <sup>-5</sup>	5	0	0	2	2	4	1	5	80	20
10 <sup>-6</sup>	5	0	1	2	0	3	2	5	60	40
10 <sup>-7</sup>	5	0	0	2	0	2	3	5	40	60
10 <sup>-8</sup>	5	0	0	0	1	1	4	5	20	80
10 <sup>-9</sup>	5	0	0	0	0	0	5	5	0	100
10 <sup>-10</sup>	5	0	0	0	0	0	5	5	0	100

the results obtained, it's concluded that 100 µg/mL concentrations of CuO NRs were effective against NDV viral growth.

### Haemagglutination Test (HA Test)

In haemagglutination assay, negative control and eggs treated with 100µg/mL concentrations of CuO NRs showed HA negative results up to 2<sup>10</sup> dilutions. In contrast, results for positive control eggs showed HA positive results up to 2<sup>10</sup> dilutions. The results indicated a significant effect of nanoparticles in preventing the growth of NDV in the allantoic fluid of treated eggs in a dose-dependent manner.

### Conclusions

CuO nanorods were extracted from *Momordica charantia* fruit extract which is an environmentally friendly and cost-effective method. TEM analysis was used to study the sizes of

nanoparticles, where it was found that the diameter of the CuO NRs was 61.48± 2 nm and the length ranged from 400–500 nm. Single crystalline and uniformly structures have been seen through XRD and SAED patterns. The nanoparticles were confirmed by UV-Vis spectrum FTIR and EDX results. Moreover, the results of physicochemical characterizations of CuO NRs also supplemented in vitro studies observations. The green synthesized CuO NRs find potential applications in the field of nanomedicine and could be used to develop targeted therapies against bacteria, fungi and viruses. The diameters of the prepared CuO NRs were smaller than the pores of the bacterial cell walls, and therefore the effect of these minutes lies in their effect on the enzymatic activities inside the cells, thereby inhibiting the growth of the bacteria. The therapeutic potential of CuO NRs against *Corynebacterium xerosis*, *Streptococcus viridians* and R<sub>2</sub>B strain of Newcastle disease is reported for the first time.

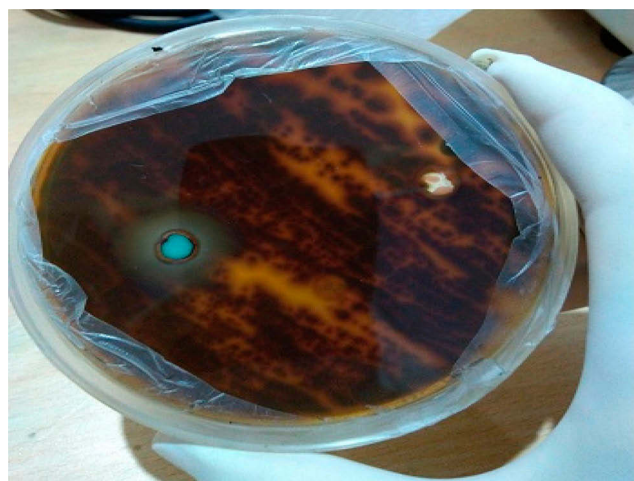


**Figure 10** Antifungal activity of CuO nanorods against *Trichophyton rubrum*.

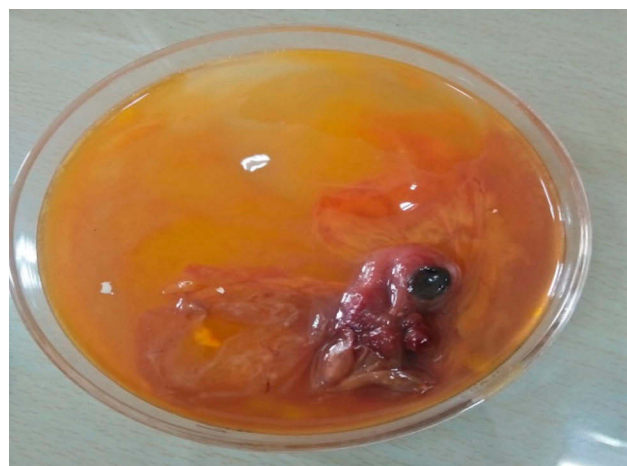


**Figure 11** In ovo antiviral activity of CuO nanorods against R<sub>2</sub>B strain of Newcastle disease virus.

*C. xerosis* and NDV, both are reported to cause conjunctivitis in humans; CuO NRs are found to be quite effective against both in vitro and in ovo method; thus for conjunctivitis, CuO NRs might provide a better solution in future after evaluating its toxic effects. Moreover, the present study enables researchers not only to design pilot-scale protocols for sustainable nanoparticle synthesis from natural resources by a simple method but also promotes to screen their antimicrobial or antiviral potential. As compared to other nanometals there are very few studies reported on interactions of microbes with copper nanoparticles. So, by exploring the mechanisms of interaction of CuO NRs on long-term antimicrobial efficacy, they could open up new avenues in the field of nano-medicine.

## Acknowledgments

Authors are highly thankful to Prof. Rizwan Hasan Khan (Interdisciplinary Biotechnology Unit, AMU, Aligarh), Dr. Azizur Rehman (Department of Saidla, AMU, Aligarh), Mr. Mohammad Furquan (IIT Bombay), Dr. Absar Ahmed (Director, Interdisciplinary Nanotechnology Unit, AMU, Aligarh), Mr. Ashraf Ali & Dr. Afsar Hussain Rizvi (Interdisciplinary Nanotechnology Unit, AMU, Aligarh), Dr. Ateeq (Physics department AMU, Aligarh), Dr. Reshma (Chemistry department AMU, Aligarh), Dr. Hashim (Applied Physics, AMU, Aligarh) and Dr Kamil Hussain (Assistant Professor in Chemistry, Rohelkhand University) for their valuable guidance provided in physiochemical characterization of sample. In addition, authors gratefully acknowledge USIF and Interdisciplinary Nanotechnology Unit of A. M.U, Aligarh. Part of this study belongs to the PhD work of the first author Ms Hina Qamar.

## Disclosure

The authors report no conflicts of interest in this work.

## References

- Dahoumane SA, Jeffryes C, Mechouet M, Agathos SN. Biosynthesis of inorganic nanoparticles: a fresh look at the control of shape, size and composition. *Bioengineering*. 2017;4(14):1–16. doi:10.3390/bioengineering4010014
- Oberdorster G, Oberdorster E, Oberdorster J. Nanotoxicology: an emerging discipline evolving from studies of ultrafine particles. *Environ Health Perspect*. 2005;113(7):823–839. doi:10.1289/ehp.7339
- Karlsson HL, Gustafsson J, Cronholm P, Moller L. Size dependent toxicity of metal oxide particles – a comparison between nano- and micrometer size. *Toxicol Lett*. 2009;188(2):112–118. doi:10.1016/j.toxlet.2009.03.014
- Nasrollahzadeh M, Mohammad S, Sajadi Rostami A, Vartooni Hussin SM. Green synthesis of CuO nanoparticles using aqueous extract of *Thymus vulgaris* L. leaves and their catalytic performance for N-arylation of indoles and amines. *J Colloid Interface Sci*. 2016;466:113–119. doi:10.1016/j.jcis.2015.12.018
- Grigore ME, Biscu ER, Holban AM, Gestal MC, Grumezescu AM. Methods of synthesis, properties and biomedical applications of CuO nanoparticles. *Pharmaceuticals (Basel)*. 2016;9(4):E75. doi:10.3390/ph9040075
- Devi HS, Singh TD. Synthesis of copper oxide nanoparticles by a novel method and its application in the degradation of methyl orange. *Adv Electr Electron Eng*. 2014;4:83–88.
- Bhattacharjee A, Ahmaruzzaman M. CuO nanostructures: facile synthesis and applications for enhanced photodegradation of organic compounds and reduction of p-nitrophenol from aqueous phase. *RSC Adv*. 2016;6(47):41348–41363. doi:10.1039/C6RA03624D
- Dagher S, Haik Y, Ayesh AI, Tit N. Synthesis and optical properties of colloidal CuO nanoparticles. *J Lumin*. 2014;151:149–154. doi:10.1016/j.jlumin.2014.02.015
- Nations S, Long M, Wages M, et al. Subchronic and chronic developmental effects of copper oxide (CuO) nanoparticles on *Xenopus laevis*. *Chemosphere*. 2015;135:166–174. doi:10.1016/j.chemosphere.2015.03.078
- Soomro RA, Sherazi STH, Memon N, et al. Synthesis of stable copper nanoparticles and their use in catalysis. *Adv Mat Lett*. 2014;5(4):191–198. doi:10.5185/amlett.2013.8541
- Le TTT, Fribourg Blanc E, Dang MC. Synthesis and optical properties of copper nanoparticles prepared by a chemical reduction method. *Adv Nat Sci Nanosci Nanotechnol*. 2011;2(1):015009. doi:10.1088/2043-6262/2/1/015009
- Mandava K, Kadimcharla K, Keesara NR, et al. Green synthesis of stable copper nanoparticles and synergistic activity with antibiotics. *Indian J Pharm Sci*. 2017;79(5):695–700. doi:10.4172/pharmaceutical-sciences.1000281
- Hyungsoo C, Sung Ho P. Seedless growth of free-standing copper nanowires by chemical vapor deposition. *J Am Chem Soc*. 2004;126(20):6248–6249.
- Huang L, Jiang H, Zhang J, Zhang Z, Zhang P. Synthesis of copper nanoparticles containing diamond-like carbon films by electrochemical method. *Electro Comm*. 2006;8(2):262–266. doi:10.1016/j.elecom.2005.11.011
- Joshi SS, Patil SF, Iyer V, Mahumuni S. Radiation-induced synthesis and characterization of copper nanoparticles. *Nanostru Mater*. 1998;10(7):1135–1144. doi:10.1016/S0965-9773(98)00153-6
- Aruldas N, Raj CP, Gedanken A. Synthesis, characterization and properties of metallic copper nanoparticles. *Chem Mater*. 1998;10(5):1446–1452. doi:10.1021/cm9708269
- Gawande MB, Goswami A, Felpin F-X, et al. Cu and Cu-based nanoparticles: synthesis and applications in catalysis. *Chem. Rev*. 2016;116(6):3722–3811. doi:10.1021/acs.chemrev.5b00482
- Havlickova B, VA C, Friedrich M. Epidemiological trends in skin mycoses worldwide. *Mycoses*. 2008;51(Suppl. 4):2–15. doi:10.1111/j.1439-0507.2008.01606.x
- Dobrowolska A, Paweł SC, Kaszuba A, Kozłowska M. PCR-RFLP analysis of the dermatophytes isolated from patients in Central Poland. *J. Dermat. Sci*. 2006;42(1):71–74. doi:10.1016/j.jdermsci.2006.01.001
- Kumar R, Shukla SK, Pandey A, et al. Copper oxide nanoparticles: an antidermatophytic agent for *Trichophyton* spp. *Nanotechnol Rev*. 2015;4(5):401–409. doi:10.1515/ntrev-2015-0010
- Nakamura K, Ohta Y, Abe Y, Imai K, Yamada M. Pathogenesis of conjunctivitis caused by Newcastle disease viruses in specific pathogen-free chickens. *Avian Pathol*. 2004;33(3):371–376. doi:10.1080/0307945042000220309
- Available from: <https://www.oie.int/en/animal-health-in-the-world/animal-diseases/Newcastle-disease/>.
- Sasidharan S, Chen Y, Saravanan D, Sundram KM, Yoga Latha L. Extraction, isolation and characterization of bioactive compounds from plants' extracts. *Afr J Tradit Complement Altern Med*. 2011;8(1):1–10.

24. Mary APA, Ansari AT, Subramanian R. Sugarcane juice mediated synthesis of copper oxide nanoparticles, characterization and their antibacterial activity. *King Saud Univ Sci*. 2019. doi:10.1016/j.jksus.2019.03.003
25. Bauer AW, Kirby WMM, Sherris JC, Turck M. Antibiotic susceptibility testing by a standardized single disk method. *Am J Clinical Pathol*. 1996;45(4):493–496. doi:10.1093/ajcp/45.4 ts.493
26. CLSI. *Performance Standards for Antimicrobial Susceptibility Testing, Fifteenth Informational Supplement, CLSI Document M100-S16*, vol 26–3; M7-A7, vol 26–2; M2-A9, vol 26–1. Wayne, PA; 2006.
27. European Directorate for the Quality of Medicines and Health Care (EDQM). *European Pharmacopoeia*. 4th ed. Strasbourg: Council of Europe; 2002.
28. Hanson RP. Newcastle disease. In: Hitchner SB, Domermuth CH, Purchase H, Williams JE, editors. *Isolation and Identification of Avian Pathogens*. New York: The American Association of Avian Pathologist. Arnold Printing Corporation, Itnaca; 1975:160–173.
29. Allan WH, Lancaster JE, Toth B. *Newcastle Disease Vaccines Their Production and Use*. No. 10. Rome: Food and Agriculture Organization of the United Nations; 1798.
30. Reed LJ, Muench H. A simple method of estimating 50 percent endpoint. *Am J Hyg*. 1938;27:493.
31. Jia S, Shen M, Zhang F, Xie J. Recent advances in *Momordica charantia*: functional components and biological activities. *Int J Mol Sci*. 2017;18(12):2555. doi:10.3390/ijms18122555
32. Kubola J, Siriamornpun S. Phenolic contents and antioxidant activities of bitter melon (*Momordica charantia* L.) leaf, stem and fruit fraction extracts *in vitro*. *Food Chem*. 2008;110(4):881–890. doi:10.1016/j.foodchem.2008.02.076
33. Nkhili E, Loonis M, Mihai S, Hajjid HE, Dangles O. Reactivity of food phenols with iron and copper ions: binding, dioxygen activation and oxidation mechanisms. *Food Funct*. 2014;5(6):1186–1202. doi:10.1039/C4FO00007B
34. Zayyoun N, Bahmad L, Laanab L, Jaber B. The effect of pH on the synthesis of stable Cu<sub>2</sub>O/CuO nanoparticles by sol–gel method in a glycolic medium. *Appl Phys A*. 2016;122(5):488. doi:10.1007/s00339-016-0024-9
35. Yugandhar P, Vasavi T, Maheswari Devi PU, Savithamma N. Bioinspired green synthesis of copper oxide nanoparticles from *Syzygium alternifolium* (Wt.) Walp: characterization and evaluation of its synergistic antimicrobial and anticancer activity. *Appl Nanosci*. 2017;7(7):417–427. doi:10.1007/s13204-017-0584-9
36. Baoshun W, Weiwei Z, Zhiyun Z, et al. Cu<sub>2</sub>O hollow structures-microstructural evolution and photocatalytic properties. *RSC Adv*. 2016;6:103700–103706. doi:10.1039/C6RA22474A
37. Eltarahony M, Zaki S, Abd-El-Haleem. D. Concurrent synthesis of zero and one-dimensional, spherical, rod, needle and wire-shaped CuO nanoparticles by *Proteus mirabilis* 10B. *J Nanomater*. 2018;2018:1–14.
38. Sanyasi S, Majhi RK, Kumar S, et al. Polysaccharide capped silver nanoparticles inhibit biofilm formation and eliminate multidrug-resistant bacteria by disrupting bacterial cytoskeleton with reduced cytotoxicity towards mammalian cells. *Sci Rep*. 2016;6(1):1–16. doi:10.1038/srep24929
39. Mamun Rashid M, Akhter KN, Chowdhury JA, et al. Characterization of phytoconstituents and evaluation of antimicrobial activity of silver-extract nanoparticles synthesized from *Momordica charantia* fruit extract. *BMC Complement Altern Med*. 2017;17(336):1–7. doi:10.1186/s12906-016-1505-2
40. Kumari P, Panda PK, Jha E, et al. Mechanistic insight to ROS and apoptosis regulated cytotoxicity inferred by green synthesized CuO nanoparticles from *Calotropis gigantea* on embryonic zebrafish. *Sci Rep*. 2017;7(1):16284. doi:10.1038/s41598-017-16581-1
41. Azam A, Ahmed AS, Oves M, Khan MS, Memic A. Size-dependent antimicrobial properties of CuO nanoparticles against gram-positive and -negative bacterial strains. *Int J Nanomedicine*. 2012;7:3527–3535. doi:10.2147/IJN.S29020
42. Fritz-Popovski F, Ludwikowska S, Köck A, Keckes J, Maier GA. Study of CuO nanowire growth on different copper surfaces gerhard. *Sci Rep*. 2019;9(1):807. doi:10.1038/s41598-018-37172-8
43. Cornell RM, Schwertmann U. *The Iron Oxides Structure, Properties, Reactions Occurrences and Uses*. Weinheim: Wiley-VCH; 1996.
44. Khan A, Rashid A, Younas R, Chong R. A chemical reduction approach to the synthesis of copper nanoparticles. *Int Nano Lett*. 2016;6(1):21–26. doi:10.1007/s40089-015-0163-6
45. Vasantharaj S, Sathiyavimal S, Saravanan M, et al. Synthesis of ecofriendly copper oxide nanorods for fabrication over textile fabrics: characterization of antibacterial activity and dye degradation potential. *J Photochem Photobiol B*. 2019;191(191):143–149. doi:10.1016/j.jphotobiol.2018.12.026
46. Murugadas A, Zeeshan M, Thamaraiselvi K, Ghaskadbi S, Akbarsha MA. Hydra as a model organism to decipher the toxic effects of copper oxide nanorod: eco-toxicogenomics approach. *Sci. Rep*. 2016;6(1):29663. doi:10.1038/srep29663
47. Auffan M, Rose J, Bottero J-Y, et al. Towards a definition of inorganic nanoparticles from an environmental, health and safety perspective. *Nat Nanotechnol*. 2009;4(10):634–641. doi:10.1038/nnano.2009.242
48. Brayner R, Ferrari IR, Brivois N, et al. Toxicological impact studies based on escherichia coli bacteria in ultrafine ZnO nanoparticles colloidal medium. *Nano Lett*. 2006;6(4):866–870. doi:10.1021/nl052326h
49. Chatterjee AK, Chakraborty R, Basu T. Mechanism of antibacterial activity of copper nanoparticles. *Nanotechnology*. 2014;25(13):135101. doi:10.1088/0957-4484/25/13/135101
50. Monteiro DR, Silva S, Negri M, et al. Silver colloidal nanoparticles: effect on matrix composition and structure of candida albicans and candida glabrata biofilms. *J Appl Microbiol*. 2012;114(4):1175–1183. doi:10.1111/jam.12102
51. Kim JH, Cho H, Ryu SE, Choi MU. Effects of metal ions on the activity of protein tyrosine phosphatase VHR: highly potent and reversible oxidative inactivation by Cu<sup>2+</sup> Ion. *Arch Biochem Biophys*. 2000;382(1):72–80. doi:10.1006/abbi.2000.1996
52. Perfect JR. The antifungal pipeline: a reality check. *Nat Rev Drug Discov*. 2017;1474:1776–1784.
53. Vandeputte P, Ferrari S, Coste AT. Antifungal resistance and new strategies to control fungal infections. *Int J Microbiol*. 2012;2012:1–26. doi:10.1155/2012/713687

## International Journal of Nanomedicine

### Publish your work in this journal

The International Journal of Nanomedicine is an international, peer-reviewed journal focusing on the application of nanotechnology in diagnostics, therapeutics, and drug delivery systems throughout the biomedical field. This journal is indexed on PubMed Central, MedLine, CAS, SciSearch®, Current Contents®/Clinical Medicine,

Submit your manuscript here: <https://www.dovepress.com/international-journal-of-nanomedicine-journal>

Dovepress

Journal Citation Reports/Science Edition, EMBASE, Scopus and the Elsevier Bibliographic databases. The manuscript management system is completely online and includes a very quick and fair peer-review system, which is all easy to use. Visit <http://www.dovepress.com/testimonials.php> to read real quotes from published authors.